Normal Mode Analysis of a Human Fibula

J.-G. Tseng[1]*, B.W. Huang[2], S.-H. Liang[2], K.T. Yen[1], Y.C. Tsai[2]

[1]Department of Leisure and Sports Management, Cheng Shiu University, Kaohsiung, Taiwan, R.O.C.
[2]Graduate Institute of Mechatronics Engineering, Cheng Shiu University, Kaohsiung, Taiwan, R.O.C.
E-mail: james.tseng@csu.edu.tw

Abstract: The human fibula is not a structural bone. It is positioned on the outer edge of the lower leg, formed part of the ankle joint and provided for stability of the lower extremity in movement. Inverse engineering technique is used to obtain a 3D complex geometry of the real human fibula by white light scanning a synthesis human fibula. Modal tests are performed to get the natural frequencies of the synthesis human fibula. The experimental data are then verified with that obtained from finite element method (FEM). After confirming the correctness of the finite element 3D synthesis human fibula model, the real human bone properties are brought into models for numerical modal analysis. Several fundamental normal modes are found. A higher frequency torsion and dilation coupled mode is also obtained to prove that the combination of bending, torsion, dilation, etc. modes can be coupled to form a normal modes.
[J.-G. Tseng, B.W. Huang, S.-H. Liang, K.T. Yen, Y.C. Tsai. **Normal Mode Analysis of a Human Fibula.** *Life Sci J* 2014;11(12):711-718]. (ISSN:1097-8135). http://www.lifesciencesite.com. 133

Keywords   Human fibula, normal mode, experiments, FEM.

1. Introduction

The fibula does not reach up as far as the knee joint; rather, its lower portion, including the specialized groove and tendon mechanism, forms part of the ankle joint, allowing for stability in movement. This is due to the fibula's major role as an anchor point for the various muscles and ligaments of the leg and ankle. The fibula is not a structural bone and it is positioned on the outer edge of the lower leg. Because of this, it is sometimes used as donor stock for bone grafts. But knee or ankle injuries are the most encountered cases in sporting and physical activities. These injuries have affected the knee or ankle joints and ligaments severely even transform into the chronic disease.

Cornelissen, et al. [1] examined the influence of soft tissues and joints on the vibration of the human tibia by modal analysis on amputated lower limbs, where the soft tissues and the fibula were dissected gradually. The fibula was found to have a stiffening effect on the tibia. Scaglioni et al. [2] discussed The role of the fibula head flap for joint reconstruction after oasteoarticular resection.

Rutten et al. [3] investigated how LIPUS affects bone healing at the tissue level in patients with a delayed union of the osteotomized fibula, by using histology and histomorphometric analysis to determine bone formation and bone resorption parameters. suggest that LIPUS accelerates clinical fracture healing of delayed unions of the fibula by increasing osteoid thickness, mineral apposition rate, and bone volume, indicating increased osteoblast activity, at the front of new bony callus formation.

Bediz et al. [4] observed the structural dynamic property changes of the tibia extracted from the vibration analysis data. bone mineral density and vibration measurements were made both in in vivo and in vitro conditions. The relationship between structural dynamic properties, obtained and bone mineral densities measured were investigated. Also, the effect of soft tissues on measured structural dynamic properties was analyzed.

Seikaly et al. [5] mentioned that the major advantage of osseous free flaps in head and neck reconstruction is the potential of implants which would aid oral or craniofacial rehabilitation. The fibula is the most commonly used bone in these reconstructions. Bone impacted fibulas (BIF) were found to have a higher marrow bone density when it is compared to the unmodified fibular free flaps. Lower degree of dental implant vibration was observed in the BIF and compared to original fibulas. All modified fibular free flaps survived in the study.

Brooke and McIlroy [6] investigated the afferent source of a human lower limb reflex that spans two joints and may link limb muscular activity during movement. Low threshold (motor nerve threshold (MT) to 1.6 MT) single, 1 msec, pulses were delivered to the common personal nerve at caput fibula.

Hetsroni and Mann [7] reviewed the literature and proposed that the fibula stress fractures should be managed with rest from any precipitating activity, physical therapy, and treatment of any contributing factor, whether metabolic, nutritional, postural, or other.

Pacifico et al. [8] discussed that the pattern of load-bearing in the tibia increases following the removal of the fibula. A further contribution to the

problem may be a degree of relative ischaemia as a result of the harvest of the personal artery.

Sherbondy and Sebastianelli [9] discussed that the stress fractures of the medial malleolus and distal fibula typically affect the athletic and running population and manifest the usual signs and symptoms of stress fractures. Axial and torsional forces, muscular contractions, and alignment are believed to play a role in their development.

Stress fractures are often confused with malignancy or osteomyelitis. Distal fibula stress fractures are usually seen in distance runners or dancers. Anand and Asumu [10] reported a case of bilateral distal fibula stress fractures in a 9-year-old girl caused by roller blade boots.

Pekedis et al. [11] developed an ankle model (tibia, fibula, calcaneus, and talus) with computer tomography and the finite element method was applied to analyze the stresses and strains occurred in ligaments and bones for four different positions (10° dorsiflexion, 0° neutral position, 10° plantar flexion, 20° plantar flexion).

Faustini et al. [12] acquired the geometry of the residual limb, liner and socket from computed tomography (CT) data of a transtibial amputee. Three different compliant designs were analyzed using finite element method (FEM) to assess the structural integrity of the sockets and their ability to relieve local pressure at the fibula head during normal walking.

Cheung and Zhang [13] developed a 3D finite element model of the human ankle-foot complex and a custom-molded insole from 3D reconstruction of magnetic resonance images (MRI) and surface digitization. The distal tibia and fibula, together with 26 foot bones and 72 major ligaments and the plantar fascia, were embedded in a volume of soft tissues. Badawi et al. [14] used MRI image enhancements using different contrast agents. And considered the magnetized-saline (MS) as a new MRI brain contrast agent (CA). Leading to the result; magnetized saline injection affect signal intensity and enhance contrast in MRI brain images.

Guo et al. [15] measured the quadriceps forces along with varied squat angles and built a simplified three-dimensional finite element model, including tibia, fibula, patella, ligaments and quadriceps tendon. Then, the contact pressure of knee joint was analyzed for the squat with the established model of knee joint involving the obtained quadriceps forces from finite element analysis.

Huang et al. [16] examined the fundamental dynamic characteristic of both the solid and hollow femur, experimentally and numerically. Then, they are imported to the finite element package, ANSYS, to perform the analysis. Huang et al. [17] investigated the dynamic property of cranium by experimental and theoretical analysis through skull model made in polystyrene. Reverse engineering analysis is adopted to build up geometric 3D skull CAD model by transferring this 3D skull CAD model into ANSYS (FEA package) acceptable model.

This research studies the fibula of the human lower extremity structure via experimental modal test and vibration modal analysis by FEM. The FEM is a powerful tool in the simulation of living structures. Using of noninvasive methods such as finite element method can help to determine the dynamic behavior of fibula, knee, ligament, etc., before the treatment (such as anterior drawer test and posterior drawer test) applied to the patients. To understand the dynamic characteristics of the human fibula structure will help to operative need and even avoid injuries.

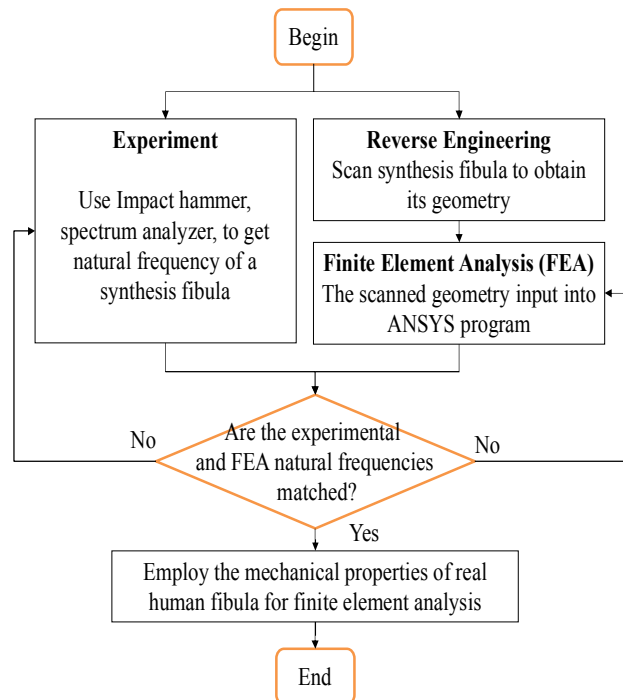Figure 1. A teaching synthesis human fibula (made by polypropylene)

Figure 2. Flow chart of the human fibula analysis

2. Methodology

It is hard to obtain the geometry of real human fibula. A typical teaching synthesis human fibula made by plastic material, polypropylene, bought from 3B Incorporation, is shown in Figure 1. The procedure of this research includes three major parts, reverse engineering, experiment and finite element analysis, etc. as shown in the flow chart in Figure 2 and will be described in the following subsections.

2.1 Reverse Engineering

As computer-aided design (CAD) has become more popular, reverse engineering (RE) has become a viable method to create a 3D virtual geometry of an existing physical component for use in three dimensional CAD, CAM, CAE or other software [18]. The reverse engineering process involves measuring an object, reconstructing it as a 3D model, manufacturing the mold and product. The physical object can be measured using 3D scanning technologies like laser scanners, structured light digitizers, CMMs (Coordinate Measuring Machine), or computed tomography. The measured data alone, usually represented as a set of points, lacks topological information and is therefore often processed and modeled into a more usable format such as a set of NURBS surfaces, a triangular-faced mesh or a CAD model. Reverse engineering is also used by businesses to bring existing physical geometry into digital product development environments, to make a digital 3D record of their own products or to assess competitors' products. It is used to analyze, for instance, how a product works, what it does, and what components it consists of, estimate costs, and identify potential patent infringement, etc.

The reverse engineering is employed by using scanner to obtain the outer profile of a teaching synthesis human fibula. In this study, 3D white light four-axis laser scanner is used to build the geometry of the plastic fibula in reverse engineering sense. The plastic fibula is placed on the four-axis laser scanner platform for 3D digital scanner to scan and measure. The scanning process requires overlaps of scanned dots in different directions, coordinate and matrix transformation in order to complete the modeling.

Because the surface of just created model from 3D digital scanner is very rough and have a bunch of little holes. This built model will be imported into automated reverse engineering software, Geomagic Studio, to precede multiple repairing, patching and smoothing of the surface for the 3D model. When the model meets the 3D geometric smooth requirements without any hole, it will be transmitted to finite element software ANSYS for modal analysis [19].
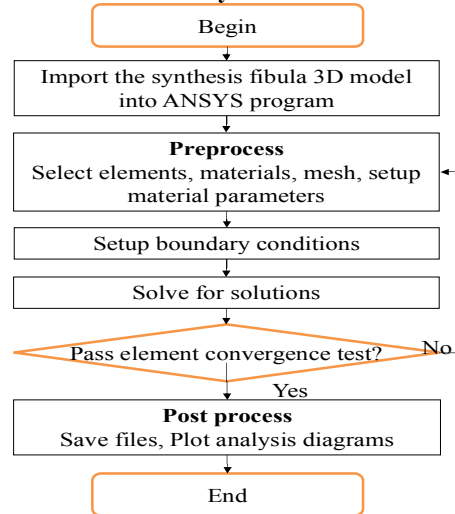
2.2 Finite Element Analysis

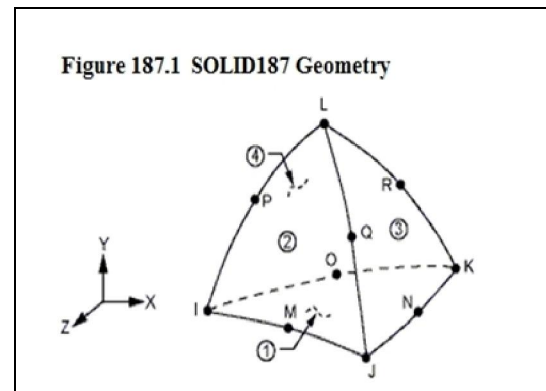Figure 3. Flow chart of the finite element analysis

Figure 4. Geometry of ANSYS Solid187 element

In this study, the finite element (FE) software ANSYS is employed to analyze the dynamic characteristics of a human fibula [9]. Various ANSYS software analyzers are used to identify the natural vibration frequency, amplitude intensity. Because real human fibula is not easy to get, a synthesis polypropylene fibula manufactured by 3B products company is used to establish geometric model for the FE analysis and experimental verification with the correctness of the model. Once the FE model of the synthesis fibula is confirmed to be accurate, the parameters of real human bone are used to carry on the normal mode analysis. Figure 3 is a flow chart of finite element analysis. After import 3D fibula model into ANSYS software, select element and material, mesh, setup boundary condition, it can be solved for the solution. It should be noted that the size, shape, and its sparse density of the element will affect the accuracy of the analysis. The wisdom of using ANSYS grid established technology will strengthen the ability of grid elements, analytical precision and accuracy.

Element type Solid187 is selected for this study as shown in Figure 4. This element is a 3D solid element and an entity does not need to set the structure constant (Real constant). Solid187 is a three-dimensional 10-node entities. Each node has displacement in x, y, z direction, i.e. 3 degrees of freedom. This element has a secondary displacement and is suitable for irregular grid. It also possesses plasticity, hyper-elasticity, strengthen stress, large deformation, large strain characteristics, etc. And it can reduce the poor precision problem caused by auto mesh. The mesh diagram of a synthesis human fibula is shown in Figure 5. It can be easily seen that the boundary condition of the synthesis human fibula is free at both end which is conformed to that in experimental setup.
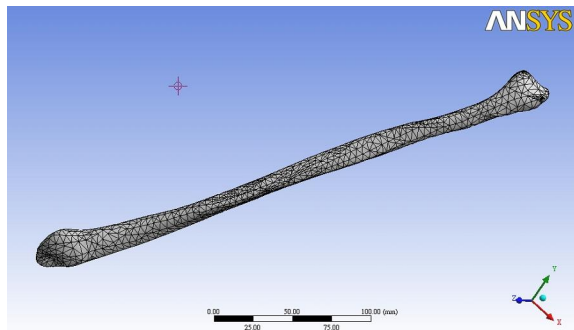
Figure 5. Mesh diagram of a synthesis human fibula.

Table 1. Material properties of 3B polypropylene synthesis human fibula

Mechanical properties	values
Young's modulus	1.3 GPa
Poisson's Ratio	0.42
Density	950 Kg/m^3

The mechanical properties, Young's modulus, Poisson's ratio and density, of the 3B polypropylene synthesis human fibula are shown in Table 1.

2.2.1 Convergence Analysis

Dynamic convergence analysis is performed for the synthesis human fibula by examine the convergence of fundamental natural frequency to find the best elements of size for the dynamic analysis. If the convergence analysis diagram presents a divergence phenomenon, one must return to pre-treatment section, adjust the settings of material parameters, contact conditions, or boundary conditions, and begin to re-analyze again. The fundamental natural frequency is converged to 26.49Hz when the number of elements near 7,200, as shown in Figure 6. Therefore, 7,236 elements are used for the following FE analysis, as shown in Table 2.

Table 2. Number of elements and nodes selected in ANSYS for 3B polypropylene synthesis human fibula

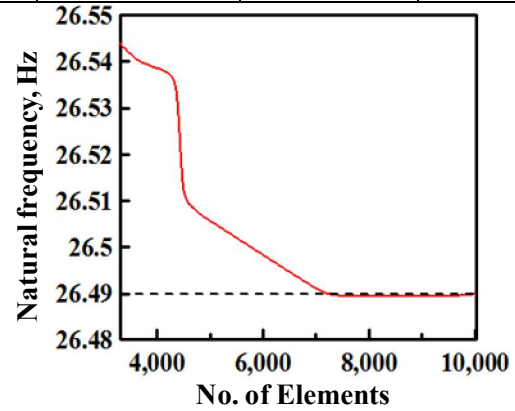| Model	Number of elements	Number of nodes	Element type
Fibula	7,236	13,370	Solid 187

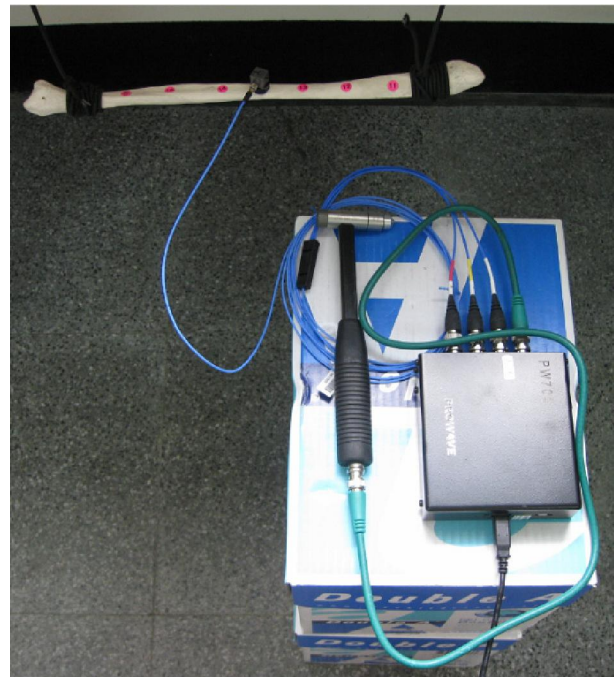Figure 6. Convergence test of a human fibula

Figure 7. The human fibula is set at free-free position with 3 axes accelerometer and an impact hammer by using PW700 spectrum analyzer experimentally.

2.3 Experimental Analysis

Impact vibration experiments are conducted for synthesis human fibula in order to obtain its vibration characteristics including natural frequencies and mode shapes. The equipment used in the experiment includes PW 700 spectrum analyzer, PC computer, impact hammer, 3-axis accelerometer, etc., as shown in Figure 7. The surface geometry of fibula is very complicated and its dimension is much smaller than femur or tibia.

The synthesis fibula is hung in the air as free-free boundary condition. Twelve experimental hit positions are marked on both front and side surfaces of the fibula. Each surface has six impact positions which are separated by 5 cm. The tri-axial accelerometer is fixed in the middle of the fibula for contentment of measuring data. Three hit points are marked for the impact hammer on each side of the accelerometer. The experiment setup schematic diagram of the front side of the fibula is shown in Figure 8. Since the synthesis fibula is thin, flat, soft and no uniform in shape, the hit positions (red dots in Figure 7) are not in the same plane. Therefore, it is very hard to perform the impact modal tests.
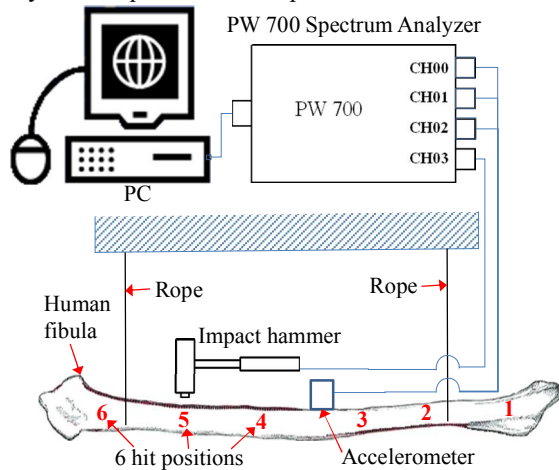

Figure 8. Experimental setup for modal test of a synthesis human fibula (front side) with six hit positions for impact hammer and one fixed position for accelerometer.
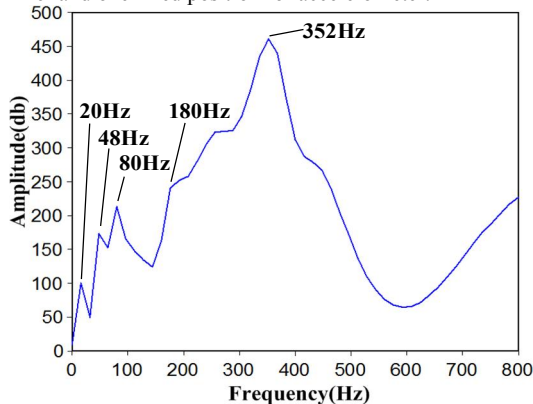

Figure 9. The experimental frequency spectrum of a synthesis human fibula.

Table 3. Comparison between measured and FEM natural frequencies

	Measured natural frequency (Hz)	Natural frequency from FEM (Hz)	Error (%)
1	20	26.5	24.5
2	48	38.1	20.0
3	80	78.9	1.4
4	180	172.8	4.2

To reduce the error of measuring data, the spectrum analyzer is set to get average response from couple of hits. After A large number of tests, several fundamental natural frequencies are found in the spectrum within 800Hz as shown in Figure 9.

2.4 Comparison between finite element and experimental analysis

The modal analysis simulation results are verified with the experimental data to make sure the accuracy of the FEM model. Four fundamental natural frequencies are compared between measured and FEM natural frequencies as shown in Table 3. The first mode is measured 20 Hz against to FEM 26.5 Hz with 24.5% error. The second mode is measured 48 Hz against to FEM 38.1 Hz with 20.0% error. This might due to the flat, soft, and irregular shape of the synthesis human fibula and cause bigger error in the experiment for measuring lower modes. Except the higher error percentage of the first two modes, the rest of the modes are within 5% error percentage. Therefore the 3D finite element model is acceptable and ready for replacing real human bone properties, Young's modulus, Poisson's ratio, and density, into the material parameters in ANSYS package.

3. Results and Discussions

After confirming the correctness of the 3D human fibula finite element model, the mechanical properties of the real human fibula, Young's modulus, Poisson's ratio, density, etc., shown in Table 4, is used in the following modal analysis.

For the free-free boundary conditions at both end of the human fibula, there are six zero Hz rigid body modes, three translation modes and three rotation modes.

Table 4. Material properties of real human fibula

Mechanical properties	values
Young's modulus	17 GPa
Poisson's Ratio	0.3
Density	2132.6 Kg/m^3

Those are not interested in the study. The first four fundamental flexible body modes with different natural frequencies and the 12th mode, 173.5 Hz, 249.3 Hz, 516.2 Hz, 707.3 Hz and 3,448Hz are obtained and shown in Table 5, respectively. For easy viewing the diagram, each mode shape is shown in pairs, one unreformed and one deformed mode shape.

Table 5. Finite element simulated natural vibration frequency with mechanical properties of real human fibula.

Mode	Natural frequencies (Hz)
1	173.5
2	249.3
3	516.2
4	707.3
12	3,448.0

The original unreformed human fibula corresponded to the first mode shape is shown in Figure 10. The first flexible mode shape of real human fibula at 173.5 Hz (bending mode in x-y plane) is shown in Figure 11. The original unreformed human fibula corresponded to the second mode shape is shown in Figure 12. The second flexible mode shape of real human fibula at 249.3 Hz (bending mode in x-z plane) is shown in Figure 13.
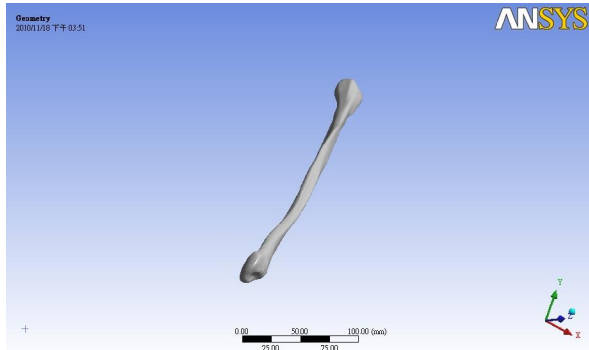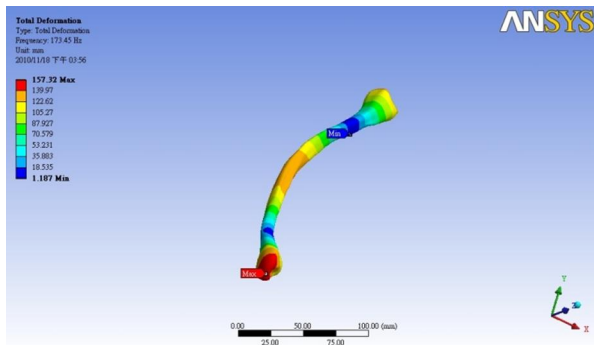

Figure 13. Second mode shape of real human fibula at 249.3 Hz (bending in x-z plane)

Figure 10. The original unreformed human fibula corresponded to the first mode shape.

Figure 14. The original unreformed human fibula corresponded to the third mode shape.

Figure 11. The first mode shape of real human fibula at 173.5 Hz (bending mode in x-y plane).
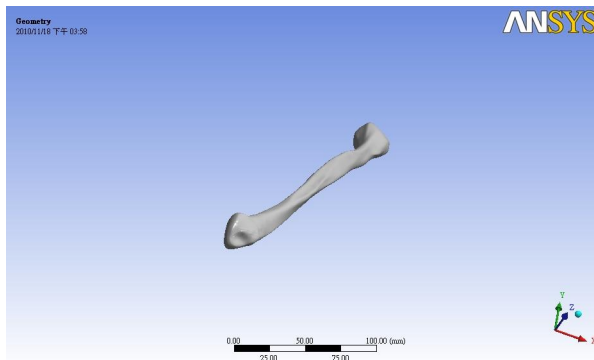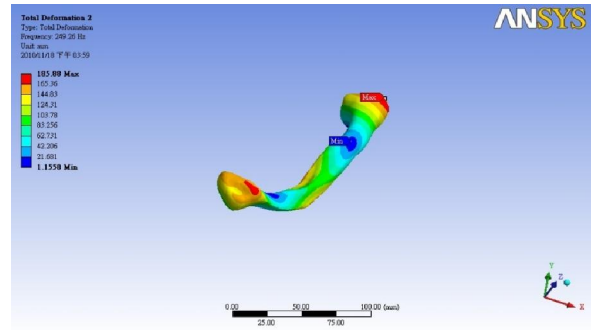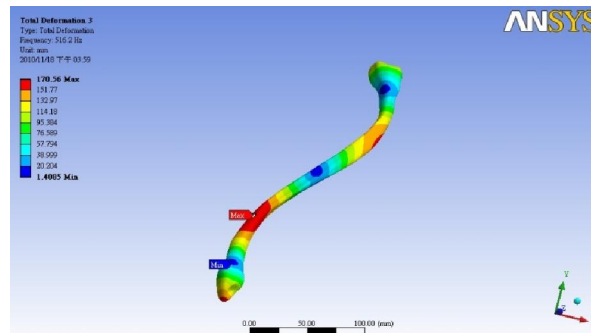

Figure 15. The third mode shape of real human fibula at 516.2 Hz (second bending mode in x-y plane).

Figure 12. The original unreformed human fibula corresponded to the second mode shape.
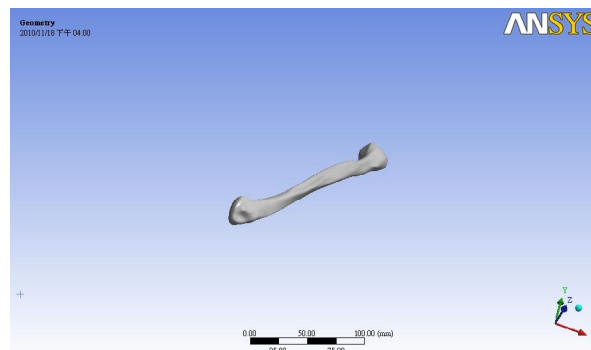

Figure 16. The original unreformed human fibula corresponded to the fourth mode shape.
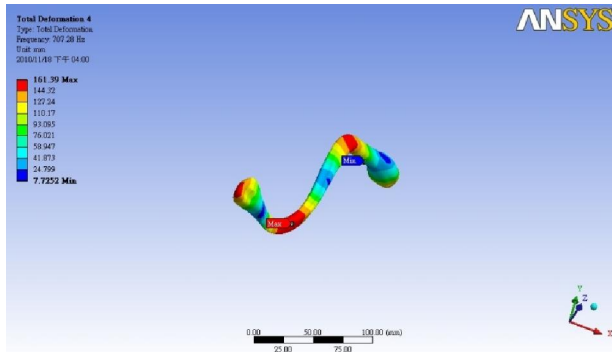
Figure 17. The fourth mode shape of real human fibula at 707.3 Hz (S shape second bending mode in y-z plane).
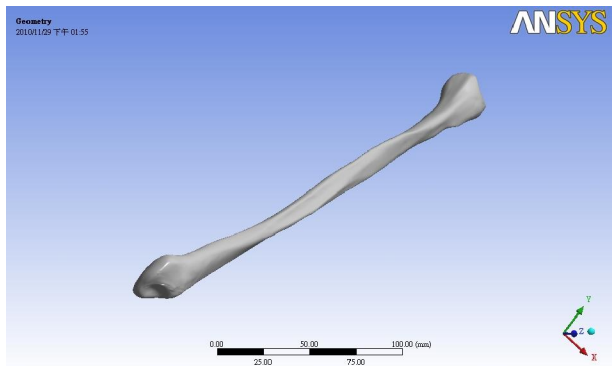

Figure 18. The original unreformed human fibula corresponded to the twelfth mode shape.
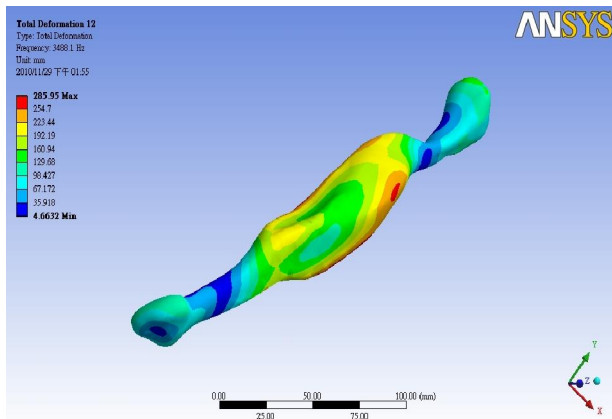

Figure 19. The twelfth mode shape of real human fibula at 3,448 Hz (Torsion and dilation combined mode in y axis).

The original unreformed human fibula corresponded to the third mode shape is shown in Figure 14. The third flexible mode shape of real human fibula at 516.2 Hz (second bending mode in x-y plane) is shown in Figure 15. The original unreformed human fibula corresponded to the fourth mode shape is shown in Figure 16. The fourth flexible mode shape of real human fibula at 516.2 Hz (S shape second bending mode in y-z plane) is shown in Figure 17.

Although the higher mode is not significant in modal analysis, the twelfth mode is still discussed here for its being a combine mode. The original unreformed human fibula corresponded to the twelfth mode shape is shown in Figure 18. The twelfth flexible mode shape of real human fibula at 516.2 Hz (Torsion and dilation combined mode in y axis) is shown in Figure 19.

4. Summary

The synthesis and real human fibula, with real bone material parameters, is studied via vibration modal analysis experimentally and numerically. Results obtained from this study are summarized as follows:

1. Reverse engineering technique is employed to obtain a 3D complex geometry of the real human fibula for finite element analysis.

2. The modal analysis simulation results are verified with the experimental data from the synthesis human fibula to make sure the accuracy of the FEM 3D model.

3. The torsion and dilation coupled mode is found. The phenomenon indicates that there exist some combinations of the pure bending, torsion, expanding/contraction modes in three dimensional FEM model.

4. The results from this modal analysis can be a helpful reference for future impact analysis, biomechanical study and medical industry applications.

References
1. Cornelissen, P., Cornelissen, M., Van der Perre, G., Christensen, A.B., Ammitzbøll, F., Dyrbye, C., 1986. Assessment of tibial stiffness by vibration testing in situ—II. Influence of soft tissues, joints and fibula. Journal of Biomechanics, 19 (7), 551-561.
2. Scaglioni, M.F., Chang, E.I., Gur, E., Barnea, Y., Meller, I., Kollander, Y., Bickels, J., Dadia, S., Zaretski, A., 2014. The role of the fibula head flap for joint reconstruction after oasteoarticular resection. Journal of Plastic, Reconstructive & Aesthetic Surgery 67, 617-623.
3. Rutten, S., Nolte, P.A., Korstjens, C.M., van Duin, M.A., Klein-Nulend, J., 2008. Low-intensity pulsed ultrasound increases bone volume, osteoid thickness and mineral apposition rate in the area of fracture healing in patients with a delayed union of the osteotomized fibula. Bone 43, 348–354.
4. Bediz, B., Özgüven, H.N., Korkusuz, F., 2010. Vibration measurements predict the mechanical properties of human tibia, Clinical Biomechanics 25, 365–371.

5. Seikaly, H., Mlynarek, A.M., Rieger, J., Harris, J.R., 2009. Bone impacted fibula (bif), a new technique of increasing bone density for placing dental implants. Oral Oncology Supplement 3, 162–200.

6. Brooke, J.D., McIlroy, W.E., 1990. Vibration insensitivity of a short latency reflex linking the lower leg and the active knee extensor muscles in humans. Electroencephalography and Clinical Neurophysiology 75 (5), 401-409.

7. Hetsroni, I., Mann, G., 2009. Fibula Stress Fractures: A Treatment Review. Operative Technique on Sports Medicine 17, 112-114.

8. Pacifico, M.D. Floyd, D., Wood, S.H., 2008. Further reporting of tibia stress fractures complicating free fibula grafts, Journal of Plastic, Reconstructive & Aesthetic Surgery, 61 (3), 346.

9. Sherbondy, P.S., Sebastianelli, W.J., 2006. Stress Fractures of the Medial Malleolus and Distal Fibula, Clinics in Sports Medicine, 25 (1), 129-137.

10. Anand, S., Asumu, T., 2005. Bilateral distal fibula stress fractures in a young child, Injury Extra, 36 (7), 280-282.

11. Pekedis, M., Ozan. F., Yildiz, H., 2011. Developing of a three-dimensional foot ankle model based on CT images and non-linear analysis of anterior drawer test by using the finite element method, Journal of Biomechanics, 44, ee14.

12. Faustini, M.C., Neptune, R.R., Crawford, R.H., 2006. The quasi-static response of compliant prosthetic sockets for transtibial amputees using finite element methods, Medical Engineering & Physics, 28, 114–121.

13. Cheung, J.T., Zhang, M., A 3-dimensional finite element model of the human foot and ankle for insole design, 2005. Archives of Physical Medicine and Rehabilitation, 86 (2), 353-358.

14. Badawi, S.M., Ahmed, W.A. EL-wafa, Kadah, Y.M., "Magnetized water and saline as a Contrast agent to Enhance MRI Images", Life Science Journal, Volume 8, Issue 1, 2011.

15. Guo, Y., Zhang, X., An, M., Chen, W., 2012. Determination of quadriceps forces in squat and its application in contact pressure analysis of knee joint, Acta Mechanica Solida Sinica, 25 (1), 53-60.

16. Huang, B.W., Huang, M.Y., Tseng, J.-G., Chang, C.H. Wang, F.-S., Lin, A.D., Tsai. Y.C., "Dynamic Characteristics of a Hollow Femur," Life Science Journal, 2012;9(1).

17. Huang, B.W., Kung, H.K., Chang, K.Y., Hsu, P.K., Tseng, J.-G. Human Cranium Dynamic Analysis. Life Science Journal. 2009; 6(4): 15–22 (ISSN: 1097 – 8135).

18. Chang, C.-C., Reverse engineering and the integration application, 1999, Gau Lih Book Co. Ltd., ISBN 957-584-664-8.

19. Kung, H.K., Huang, B.W., Chen, H.S., ANSYS and Computer Aided Engineering Analysis, 2004, Cheng Shiu University, Kaohsiung, Taiwan, R.O.C.

7/10/2014